多軸觸覺式感測器之研究
A study of multi-axial tactile sensors

計畫編號：NSC 87-2218-E-009-019
執行期限：86/08/01 - 87/07/31
主持人：黃宇中

July 31, 1998

1 中文摘要(感測器，觸覺式感測)

本研究完成一種可感測平面力的多軸觸覺式感測器結構設計，我們藉由降低感測器校準矩陣之條件因數來提生解析度，並設計一種簡單並精確的校準方法來提昇精確度。此外，本設計也做實驗驗証。

英文摘要(keyword: sensor, tactile sensing)

This work presents a new structural design for multi-axial tactile sensors to sense planar forces. Not only the resolution can be increased by reducing the condition number of calibration matrix, but also the accuracy can be enhanced by a precise and simple calibration method. And experimental results demonstrate the proposed design.

2 計畫緣由及目的

Tactile sensors can provide the contact information, e.g. force magnitude, force angle and contact point, for robotics to perform dexterous manipulation and haptic perception. Robotics research has categorised for fingertip sensors as either tactile array "extrinsic" sensing, or "intrinsic" contact sensing[1]-[2]. Intrinsic or force/torque tactile sensors, which are based on pure force/torque measurements and geometric calculations, are our concern in this work[3]-[4].

Salisbury initially proposed the feasibility of applying intrinsic contact sensing as hard finger model for finger-object interactions where forces are transmitted through only a contact[3]. Tsujimura and Yabuta reconsidered Salisbury's approach and developed an application in object detection[8]. Another research examined intrinsic contact sensing for soft fingers as to whether the finger or object has a compliant surface or both[5]. The other work has demonstrated the practical applications of intrinsic contact sensing in fingertip sensors[4][6]-[8].

Three approaches can be adopted to improve the accuracy for force/torque tactile sensors. The first approach attempts to reduce the error in the calibration matrix[9]-[10]. Many errors related to intrinsic sensing method can be traced to the inaccurate calibration[6]. The second approach attempts to reduce the condition number of calibration matrix. The word, condition number, denotes an important index for a linear system to resist external interferences. The second approach attempts to reduce the condition number of calibration matrix. The word, condition number, denotes an important index for a linear system to resist external interferences. The previous work uses an U-shape as the sensor's structure; however, it suffers a large condition number of calibration matrix up to 20.05[6]. The third approach aims to reduce the error in the electrical output vector of the strain transducers. Highly precise and expensive electronic devices for measuring the transducers' electrical outputs, e.g. voltage or resistance, are necessary particularly when the condition number of calibration matrix is large.

3 研究方法及成果

The proposed structure as depicts in Fig. 1 consists of a cylindrical fingertip, two beams with the vertical one standing at the center of the horizontal one, and a fixture. Since the sensor with the proposed structure operates in a plane, the structure can equivalently be represented as shown in Fig. 2 with the contact point of the applied force indicated by the contact angle θ. The applied force raises more significant strains on the two beams than else where; in particular, the strains on the fixed ends and joints of the two beams is larger than the rest of the beams. Therefore, the points L, R, T, U, K, and S, which are all located at the fixed ends or joints of the beams, are employed as the candidate locations for strain transducers. And we analyze the mechanical properties at these points to formulate the hard finger model of the proposed structure.

First of all, the stresses at points L, R, T, U, K, and S, are analysed. The analysis can be referred for 2-dimensional rectangle beams[7]. The x-directional component of the applied force is initially considered. Figure 3(a) pictures the equivalent structure with the fingertip and the fixture simplified while considering only the x-directional force acting on the fingertip. On the other hand, Fig. 4(a) displays the equivalent structure while considering only the y-directional component of the applied force acting on the fingertip. Moreover, the y-directional component of the applied force P_y exerts the same effect on both sides around the symmetrical axis of the structure, and the induced torque M_y has opposite effects on both sides around the structure's symmetrical axis.

Thereafter the stresses at points L, R, T, U, K and S can be found by taking the superposition of the individual stress component which has been obtained. As shown in table 1, the stresses at these points can be expressed in a linear combination of $P \cdot sin\phi$, $P \cdot sin(\theta - \phi)$, and $P \cdot cos\phi$.

In order to avoid the complexity while fully optimizing the structure, we propose a semi-heuristic way to design the flexure with the considerations on the implementation of the sensor and the reduction of the condition number.

To leave enough space for treating strain transducers on both beams, we set the half length of the horizontal beam equal to the length of the vertical beam and adjust them together to fit the space requirement. Moreover, the diameter of the fingertip is set to the length of the horizontal beam such that the width of the fingertip is consistent from top to bottom. Thus setting $a = d = r$ becomes a design constraint.

Reducing the stress variation on both beams is helpful to decrease the condition number. This can be approached by equalizing the maximum stresses on the beams. Table 2 summarizes the maximum stresses at points L, R, T, U, K and S with $a = d = r$. As a result, the maximum stresses on both beams are equal and located at points K and S when $h_2 = 1.633 \cdot h_1$.

With $a = d = r$ and $h_2 = 1.633 \cdot h_1$, the minimal condition number can be found by searching for each configuration of which the strain transducers are placed on points L, R, T, U, K and S. Figure 5 depicts the only three cases which have the three minimal condition numbers. Table 3 summarizes the results of theoretical derivations against the results of finite-element simulations by ANSYS. Since the condition numbers for the three cases are close, we evaluate them further by experiments together. For the other cases, their condition numbers are several times larger than the three cases. Here they are not included for evaluation.

As depicts in Fig. 6(a), we applied a force on the sensor by hanging a hangable weight, as shown in Fig. 6(b), down a groove on the fingertip's surface. Obviously, the force magnitude can be controlled by the weight, and the force angle depends on the orientation of the sensor. In fact, the actual contact point is shifted by the length of the groove from the desired contact point on the fingertip's surface. This phenomenon can not arise any error when the groove is oriented in the gravity direction. As a result, the accuracy of the proposed method depends on how to fabricate and orient the groove precisely. For simplicity, we recommand using only x-directional grooves for x-directional forces and y-directional grooves for y-directional forces. This is enough for calibration.

4 結論與討論

The condition number of the proposed structure is reduced theoretically and experimentally to 2.55 and 3.12, respectively[6]. The proposed calibration method has been proved for its simplicity and accuracy without any assistance of precise positioning equipments and force loads. Experimental results show that almost ±1% accuracy can be achieved. This performance is quite acceptable in practical applications. However, the grooves for applying forces are damage for the fingertip surface. This should be considered for practical applications.

Finally, the proposed structure can be further improved from two respects. First, low-cost fabrication of the sensor deserves researching. The fabrication techniques applied in MEMS shall be promising for this target. Second, the fully optimizing the proposed structure from the overall stiffness in addition relative parameters, such as condition number of calibration matrix, dynamic range, resolution is still required for advanced design work.

參考文獻

[1] P. Dario, Tactile sensing: technology and applications, *Sensors and Actuators A*, 1991, pp.251-256.

[2] R. D. Howe, Tactile sensing and control of robotic manipulation, *Journal of Advanced Robotics*, vol.8, no.3, 1994, pp.245-261.

[3] J. K. Salisbury, Interpretation of contact geometries from force measurements, *Proc. the 1st International Symposium on Robotics Research*, Bretton Woods, NH, MIT Press, Cambridge, MA, 1984, pp.565-577.

[4] A. Bicchi and P. Dario, Intrinsic tactile sensing for artificial hands, *Proc. the 4th International Symposium on Robotics Research*, Santa Barbara, CA., MIT press, Cambridge, MA, 1987, pp.83-90.

[5] A. Bicchi, Intrinsic contact sensing for soft fingers, *Proc. International Conference on Robotics and Automation*, Cincinnati,OH, 1990, pp.968-973.

[6] J. S. Son, et al, Comparison of contact sensor localization abilities during manipulation, *Robotics and Autonomous System*, vol.17, 1996, pp.217-233.

[7] X. Zhou, et al, Contact localisation using force/torque measurements, *Proc. of the IEEE International Conf. on Robotics and Automation*, Minneapolis, MA, 1996, pp.1339-1344.

[8] T. Tsujimura and T. Yabuta, Object detection by tactile sensing method employing force/torque information, *IEEE Trans. on Robotics and Automation*, vol.5, no.4, Aug. 1989, pp. 444-450.

[9] A. Bicchi and G. Canepa, Optimal design of multivariate sensors, *Measurement Science and Technology*, vol.5, no.4, 1994, pp.319-332.

[10] R. M. Voyles, et al, Shape from motion decomposition as a learning approach for autonomous agents, *Proc. of the IEEE International Conf. on Systems, Man and Cybernetics*, Vancouver, BC, Can, 1995, pp.407-412.

表格 1: Summary of the stresses at points L,R,T,U,K and S of the proposed structure in the form: $\sigma = g_1 \cdot P \cdot \sin\phi + g_2 \cdot P \cdot \sin(\theta - \phi) + g_3 \cdot P \cdot \cos\phi$.

Name of stress	comp.	g_1	g_2	g_3
$\sigma_{L,B}$	$\sigma_{Lx,B}\,\sigma_{Ly,B}$	$\frac{3}{2}\frac{h}{h_1^2}$	$\frac{3}{2}\frac{a}{h_1^2}$	$\frac{3}{2}\frac{h}{h_1^2} + \frac{1}{4}\frac{1}{h_1}$
$\sigma_{R,B}$	$\sigma_{Rx,B}\,\sigma_{Ry,B}$	$\frac{3}{2}\frac{h}{h_1^2}$	$-\frac{3}{2}\frac{a}{h_1^2}$	$-(\frac{3}{2}\frac{h}{h_1^2} + \frac{1}{4}\frac{1}{h_1})$
$\sigma_{T,U}$	$\sigma_{Tx,U}\,\sigma_{Ty,U}$	$-\frac{1}{h_2}$	$-\frac{2a}{h_2^2}$	—
$\sigma_{U,U}$	$\sigma_{Ux,U}\,\sigma_{Uy,U}$	$-\frac{1}{h_2}$	$\frac{2a}{h_2^2}$	—
$\sigma_{K,B}$	$\sigma_{Kx,B}\,\sigma_{Ky,B}$	$-\frac{3}{2}\frac{h}{h_1^2}$	$-\frac{3a}{h_1^2}$	$-(\frac{3h}{h_1^2} + \frac{3}{h_1})$
$\sigma_{S,B}$	$\sigma_{Sx,B}\,\sigma_{Sy,B}$	$-\frac{3}{2}\frac{h}{h_1^2}$	$\frac{3a}{h_1^2}$	$\frac{3h}{h_1^2} + \frac{3}{h_1}$
$\sigma_{K,U}$	$\sigma_{Kx,U}\,\sigma_{Ky,U}$	$-\frac{1}{h_2}$	$-\frac{2a}{h_2^2}$	$-\frac{6h}{h_2^2}$
$\sigma_{S,U}$	$\sigma_{Sx,U}\,\sigma_{Sy,U}$	$-\frac{1}{h_2}$	$\frac{2a}{h_2^2}$	$\frac{6h}{h_2^2}$

表格 2: Summary of the stresses at points L,R,T,U,K and S of the proposed structure with $a = d = r$.

stress	θ	ϕ	Max. stress	$h_2 = 1.633h_1$
$\sigma_{L,B}$	135°	45°	$3.00\frac{a}{h_1^2}P$	$3.00\frac{a}{h_1^2}P$
$\sigma_{R,B}$	45°	135°	$3.00\frac{a}{h_1^2}P$	$3.00\frac{a}{h_1^2}P$
$\sigma_{T,U}$	0°	90°	$0\frac{a}{h_1^2}P$	$2.00\frac{a}{h_1^2}P$
$\sigma_{U,U}$	0°	−90°	$0\frac{a}{h_1^2}P$	$2.00\frac{a}{h_1^2}P$
$\sigma_{K,B}$	0°	−90°	$4.5\frac{a}{h_1^2}P$	$4.5\frac{a}{h_1^2}P$
$\sigma_{S,B}$	180°	−90°	$4.5\frac{a}{h_1^2}P$	$4.5\frac{a}{h_1^2}P$
$\sigma_{K,U}$	90°	180°	$12\frac{a}{h_1^2}P$	$4.5\frac{a}{h_1^2}P$
$\sigma_{S,U}$	90°	0°	$12\frac{a}{h_1^2}P$	$4.5\frac{a}{h_1^2}P$

表格 3: Condition number list for the smallest three cases with $h_2 = 1.633 \cdot h_1$ from theoretical analysis, simulation and measurement.

case	stress	theory	simulation	meas.
I	$\sigma_{L,B}\,\sigma_{R,B}\,\sigma_{U,U}$	2.55	2.53	3.12
II	$\sigma_{L,B}\,\sigma_{R,B}\,\sigma_{U,U}$	3.43	3.36	3.98
III	$\sigma_{K,B}\,\sigma_{R,B}\,\sigma_{U,U}$	4.05	3.94	4.76

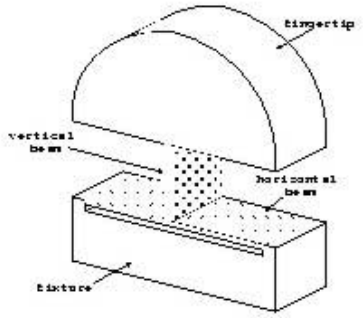

圖 1: The proposed fingertip sensor in isotropic view.

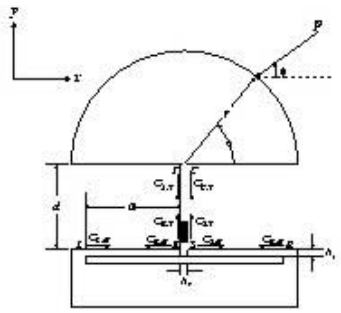

圖 2: Fingertip sensor cross section view.

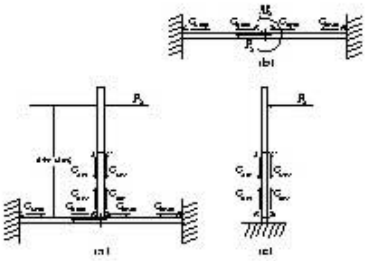

■ 3: The equivalent structures for analysis when considering the x-directional force (a) acting on the fingertip only (b) for horizontal beam only, (c) for vertical beam only.

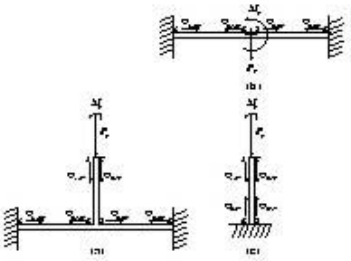

■ 4: The equivalent structures for analysis when considering the y-directional force (a) acting on the fingertip (b) for horizontal beam only, (c) vertical beam only.

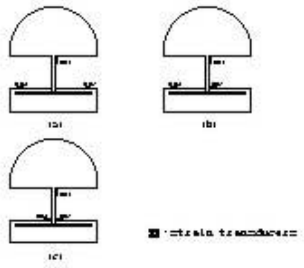

■ 5: The three cases for placing strain transducers (a) case I, (b) case II, (c) case III.

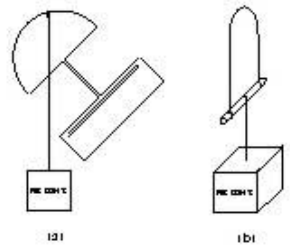

■ 6: (a) Illustration for applying a force and (b) the hangable weight.

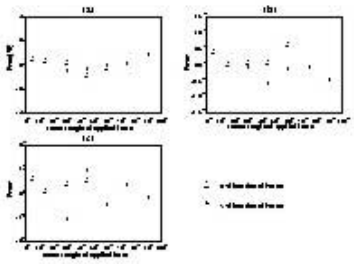

■ 7: The error plot of the measured force, for the case I (a) error of the force magnitude, (b) error of the force angle, (c) error of the contact angle.